DOI: 10.1002/chem.200701137

Polyhedral Structures with an Odd Number of Vertices: Nine-Coordinate Metal Compounds

Antonio Ruiz-Martínez, David Casanova, and Santiago Alvarez*[a]

Abstract: The stereochemistry of nine-coordinate transition-metal and rare-earth compounds has been studied by means of continuous shape measures (CShM) and related tools. Several reference nine-vertex polyhedra have been defined and their minimal distortion interconversion paths established. A theoretical shape map is presented in which the structures can be placed according to their distances in CShM space to the capped square antiprism and the tricapped trigonal prism, which are the most common polyhedra in nine-coordinate compounds. The structures of almost 2000 metal coordination spheres in molecular and extended solid-state compounds have been analyzed. Clear stereochemical trends can be established for subsets of these compounds grouped according to the nature of their ligands, which include families of compounds spread along the interconversion paths between the capped square antiprism and the capped cube, or between the tricapped trigonal prism and the tridiminished icosahedron.

Keywords: continuous shape measures · lanthanides · nine-coordinate compounds · stereochemistry · transition metals

Introduction

The definition of the spatial arrangement of a set of atoms in chemical structures, either molecular or extended, by means of the vertices of ideal polyhedra has formed part of the language of modern chemistry since the definitive introduction of the tetrahedron by Van 't Hoff and the octahedron by Werner at the end of the 19th century. Polyhedra can thus represent the metallic core of clusters or cage compounds, which are a set of ions held together by electrostatic forces and repeated periodically in an extended solid, or the coordination sphere of a particular atom in a molecule or network. Even the organization of molecular building blocks in supramolecular units is often well represented by polyhedra, which in some cases are obtained by design through the appropriate choice of the chemical groups that hold the vertex atoms in place. Although we can represent such a diversity of chemical structures in terms of a common set of ideal polyhedra, we must not forget that the relationships between vertices differ depending on the type of compound we are observing. Hence, in a cluster the polyhedral edges may correspond to chemical bonds, whereas they do not represent bonds in either supramolecular or coordination polyhedra. In coordination polyhedra the vertices are only linked indirectly through the common central atom, whereas in a supramolecular structure the vertices are usually linked by more or less elaborate chemical groups that may correspond topologically to the edges or faces.

The application of the polyhedral paradigm usually focuses on the most common structures with a small number of atoms (which form polyhedra with four to six vertices) and on those with a larger number of atoms that can be described by highly symmetric Platonic and Archimedean polyhedra with 8, 12, 20, 24, or 60 vertices. Nine-vertex structures belong to neither of these two categories and for that reason have been the object of few systematic studies. A classic book on inorganic stereochemistry published two decades ago, for instance, makes reference to only a few tens of nine-coordinate rare-earth complexes,[1] whereas the earlier stereochemical study by Guggenberger and Muetterties focused only on ten coordination compounds and three clusters.[2] A thorough review published one year later by Drew provides a wider compilation of structural data that covers almost 70 structures, but considers only the tricapped trigonal prism and the capped square antiprism as reference

[a] A. Ruiz-Martínez, Dr. D. Casanova, Prof. S. Alvarez
Departament de Química Inorgànica
and Institut de Química Teòrica i Computacional
Universitat de Barcelona
Martí i Franqués 1-11, 08028 Barcelona (Spain)
Fax: (+34) 93-490-7725
E-mail: santiago@qi.ub.es

Supporting information for this article is available on the WWW under http://www.chemeurj.org/ or from the author.

polyhedra.[3] The exponential growth of the number of known structures with nine-coordinated rare-earth or transition-metal atoms since those reviews were published is reflected by the data found in the Cambridge Structural Database (Figure 1). There are additional problems because often the experimental structures deviate to a significant

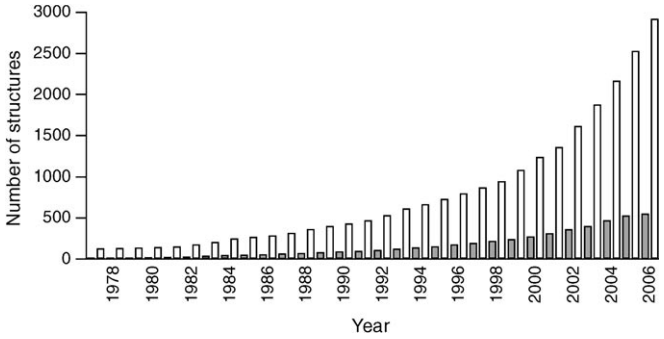

Figure 1. Evolution of the accumulated number of structures with nine-coordinated rare-earth and transition-metal atoms in the Cambridge Structural Database.

degree from the ideal shapes and also because the alternative ideal polyhedra differ from each other by small atomic displacements, which therefore, makes the assignment of a polyhedral shape to a structure complicated.

To facilitate a better structural description of nine-coordinate structures and to search for general trends in their stereochemistry, we present herein a systematic study in which we first propose a variety of reference nine-vertex shapes, which include Johnson polyhedra[4] and other less regular shapes found in chemical structures. Second, we analyze the structural characteristics of nine-coordinated metal atoms in coordination compounds and extended solids within the framework of the continuous shape measures (CShMs) approach. A related analysis of nine-vertex clusters and enneanuclear supramolecular assemblies form a second part of this work and will be reported independently.

Abstract in Spanish: *Se presenta un estudio estereoquímico de compuestos nonacoordinados de metales de transición y tierras raras, desde el punto de vista de las Medidas Continuas de Forma (CShM) y las herramientas que de ellas se derivan. Se han definido diversos poliedros de referencia de nueve vértices y se han establecido sus caminos de interconversión de mínima distorsión. Se presenta un mapa de forma teórico en el que se pueden ubicar las estructuras según su distancia en el espacio CShM al antiprisma cuadrado cofiado y al prisma trigonal tricofiado, los poliedros más comunes en compuestos nonacoordinados. Todo ello se ha aplicado al estudio de cerca de 2.000 estructuras de esferas de coordinación en compuestos moleculares y en estructuras infinitas de sólidos. Para algunas familias de compuestos, agrupados según el tipo de ligandos coordinados al metal, se pueden establecer tendencias estereoquímicas claras, como aquellos que se encuentran a lo largo de los caminos de interconversión entre el antiprisma cuadrado cofiado y el prisma trigonal tricofiado, o entre el prisma trigonal tricofiado y el icosaedro tridisminuido.*

Results and Discussion

Continuous shape measures (CShMs): Following the proposal by Avnir and co-workers[5,6] to consider symmetry and polyhedral shape as continuous properties that can be quantified from structural data, we have applied these concepts and the associated methodology to the stereochemical analysis of very large sets of molecular structures, which includes systems with four-,[7] six-,[8] seven-,[9] and eight-vertex[10] polyhedra. The so-called CShMs approach[5,11] essentially allows one to numerically evaluate by how much a particular structure deviates from an ideal shape (e.g., a polyhedron). The CShM of a set of N atoms (in the present case $N=9$ for empty polyhedra and $N=10$ for centered polyhedra) relative to a polyhedron P, characterized by their position vectors $\{\boldsymbol{Q}_i\}$, is defined by Equation (1):

$$S_{\mathrm{Q}}(\mathrm{P}) = \min \frac{\sum_{i=1}^{N} |\boldsymbol{Q}_i - \boldsymbol{P}_i|^2}{\sum_{i=1}^{N} |\boldsymbol{Q}_i - \boldsymbol{Q}_0|^2} 100 \qquad (1)$$

in which $\boldsymbol{P}_i$ are the position vectors of the corresponding vertices in reference polyhedron P and $\boldsymbol{Q}_0$ is the position vector of the geometrical center of the problem structure. The minimum is taken for all possible relative orientations in space, isotropic scaling, and for all possible pairings of the vertices of the problem and reference polyhedra. As a consequence, two shapes are identical within the CShMs approach if they differ only in size and/or orientation in space. For the study of coordination compounds, only those vertex permutations that leave the metal atom in the center of the polyhedron are considered. With such a definition, $S_{\mathrm{Q}}(\mathrm{P})=0$ corresponds to structure Q fully coincident in shape with reference polyhedron P. Larger $S_{\mathrm{Q}}(\mathrm{P})$ values correspond to larger distortions of Q from P, in which $S_{\mathrm{Q}}(\mathrm{P})=100$ is the upper limit that corresponds to the hypothetical case in which all atoms of Q occupy the same point in space.

A particular advantage of such an approach is that structures that cannot properly be described by an ideal polyhedron may in some instances be described as being along the path for the interconversion of two such polyhedra, which takes advantage of our definition of the minimal distortion interconversion pathways and the corresponding path deviation functions,[12] and are discussed briefly below.

Nine-vertex reference polyhedra: Prior to the stereochemical analysis of a variety of chemical structures, it was necessary to define the ideal shapes that we may use to describe

nine-vertex polyhedra. As there are no Platonic, Archimedean, or Catalan polyhedra with nine vertices, and as no prisms or antiprisms can be made with an odd number of vertices, the only semiregular three-dimensional figures we may consider are the octagonal pyramid, the heptagonal bipyramid, and five Johnson polyhedra. These are the capped cube (J-CCU), the capped square antiprism (J-CSAPR), the tricapped trigonal prism (J-TCTPR), the tridiminished icosahedron (J-TDIC), and the triangular cupola (J-TC).[13] As these polyhedra[4] have by definition all edges of the same length, they may be suitable to describe the structures of clusters or polynuclear complexes in which edges correspond to metal–metal bonds (or metal-bridging ligand–metal sequences). In contrast, in coordination compounds it is the vertex-to-center distance that is approximately the same for all vertices, a feature not necessarily compatible with identical edge lengths. Therefore, we will use spherical versions of the Johnson polyhedra for coordination compounds in this work, but the ideal Johnson geometries for future analysis of clusters and polynuclear complexes. We note that if the capping atoms are just added on top of the capped polyhedron in such a way that its distance to the center of the polyhedron is the same as that of the other vertices, then the capping edge lengths are much shorter than the rest of the polyhedral edges. In other words, the ideal polyhedra should relax after capping in such a way as to have comparable edge lengths, although this occurs at the cost of the regular polygonal nature of some or all of the faces. These "relaxed" polyhedra, which are defined with the help of a hard spheres model, will be used here as ideal shapes and will be identified by the prefix **r**, whereas the "unrelaxed" spherical versions that may be used in some instances for convenience will be labeled with the prefix **s** and the Johnson versions (regular polygonal faces, all edges of the same length but not spherical) with the prefix **J**. The characteristics of these nine-vertex polyhedra are summarized in Table 1, together with the abbreviations used in this paper.

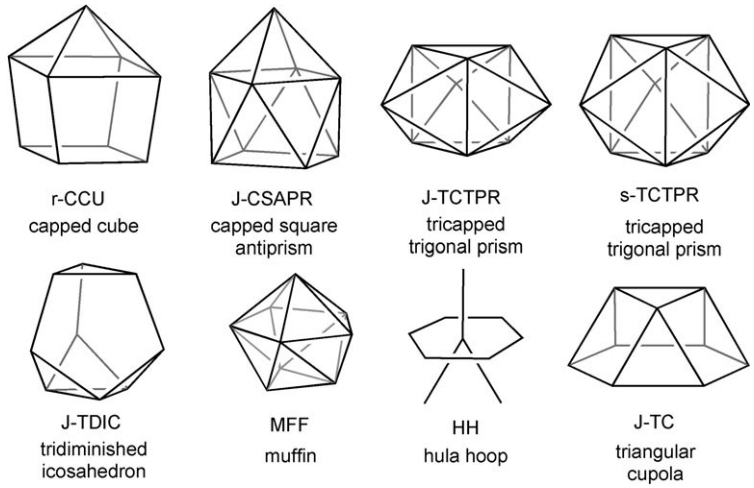

A systematic notation for describing both regular and irregular polyhedra implies grouping the vertices into sets that are related by pseudosymmetry rotation axes and expressing the number of atoms in each set. Thus, both the CCU and the CSAPR can be described as 1:4:4 polyhedra, whereas the TDIC and the TCTPR can be described as 3:3:3 figures. This notation indicates that in each case there are three sets of vertices related by tetragonal and trigonal axes, respectively. The irregular muffin (MFF) shape that will be used below does not have a symmetry axis, but it has a set of three vertices related by a two-fold pseudosymmetry axis, another set of five vertices related by a colinear five-fold pseudosymmetry axis, and the remaining vertex is sitting on this axis. Therefore, we describe the MFF as a 1:5:3 and the hula hoop (HH) as a 1:6:2 polyhedron. With this scheme it is easy to realize that the 4:5 and 2:5:2 arrangements represent two missing polyhedra in our reference set. The former could be found in complexes with rigid

Table 1. Names, abbreviations, and main characteristics of the ideal nine-vertex shapes used in this work.

Ideal shape	Abbreviation[a]	Symmetry	Vertices	Edges
triangular cupola	J-TC	C_{3v}	3:6	equivalent
tricapped trigonal prism	J-TCTPR	D_{3h}	3:3:3	equivalent
(spherical version)	s-TCTPR			dissimilar
	r-TCTPR			hard spheres
capped square antiprism	J-CSAPR	C_{4v}	1:4:4	equivalent
	s-CSAPR			dissimilar
	r-CSAPR			hard spheres
muffin	MFF	C_{2v}	1:5:3	hard spheres
capped cube -Johnson	J-CCU	C_{4v}	1:4:4	equivalent
-spherical	s-CCU			dissimilar
-relaxed	r-CCU			hard spheres
hula hoop	HH	C_{2v}	1:6:2	hard spheres
tridiminished icosahedron	TDIC	C_{3v}	3:3:3	equivalent
heptagonal bipyramid	HBPY	D_{7h}	1:7:1	
pentagonal cupola[b]	PC		4:5	

[a] The prefix J indicates a Johnson polyhedron, whereas the prefix s indicates the corresponding spherical version and r corresponds to the spherical relaxed (hard spheres) structure. [b] The nine-vertex cupola with a pentagonal base is an irregular polyhedron that should not be confused with the Johnson 15-vertex pentagonal cupola.

pentadentate macrocyclic ligands or in mixed sandwich complexes with π-bonded cyclobutadienediide and cyclopentadienide ligands, a family formed by more than 200 structures, but with a significantly elongated shape because the pentagonal and tetragonal faces correspond to chemical bonds, although these two polygons are at a nonbonding distance and are connected through a metal atom. So far we have not found any coordination compounds that could be described as 2:5:2 polyhedra.

The TC can be considered as hemispherical in the sense that it is derived from the spherical Archimedean cuboctahedron by removing the vertices from one of the hemispheres. For this reason it is not appropriate for coordination spheres and no structures with such a geometry have been found in this study.

Interconversion pathways and shape maps: In a CShM structural analysis of a given molecule, we can compare the measures obtained with respect to the different ideal polyhedra and decide which of them best describes the molecular geometry merely by choosing the smallest CShMs value. This numerical value also gives an indication of how distorted the structure is from the reference shape. Let us consider some simple examples. In considering the PuN_9 group in the $[Pu(NCMe)_9]^{3+}$ ion, we can visually recognize its CSAPR shape (Figure 2), a fact that is automatically revealed by the small value of the corresponding shape measure, S(r-CSAPR) = 0.07. The structure of the $[Nd(H_2O)_9]^{3+}$ ion,[14] however, is hard to classify as either a CSAPR or as a TCTPR. Its shape measures relative to the two ideal polyhedra, S(r-CSAPR) = 0.39 and S(r-TCTPR) = 0.40, tell us that it is equidistant from them. In a case such as this we could use the definitions of the minimal distortion pathway and the path deviation function[12] to see whether or not our structure actually belongs to the interconversion path between those two reference shapes.

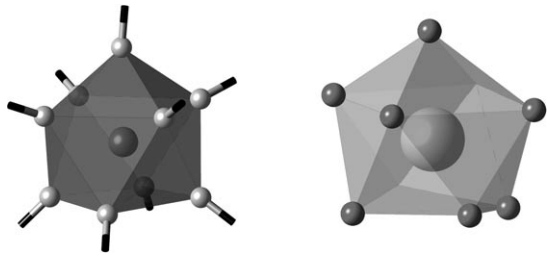

Figure 2. r-CSAPR coordination sphere of the plutonium ion in the $[Pu(NCMe)_9]^{3+}$ complex[15] (left) and distorted r-CSAPR geometry of the $[Nd(H_2O)_9]^{3+}$ cation (right).[14]

A minimal distortion pathway between two reference shapes can be defined in terms of CShMs.[12] The path deviation function, on the other hand, tells us whether a molecular structure lies along that path, or more precisely, by how much it deviates from it. Thus, we can measure such a deviation if we know its shape measures relative to two reference polyhedra. This is done by calculating the path deviation function presented in Equation (2), which calibrates the deviation of structure X from the minimal distortion interconversion pathway between reference shapes P and T. The values of the mutual shape measures between pairs of ideal polyhedra, $S_P(T)$, are presented in Table 2.

$$\Delta_X(P,T) = \frac{1}{\operatorname{asin}\frac{\sqrt{S_P(T)}}{10}}\left[\operatorname{asin}\frac{\sqrt{S_X(P)}}{10} + \operatorname{asin}\frac{\sqrt{S_X(T)}}{10}\right] - 1 \qquad (2)$$

According to the definition given in Equation (2), the deviation from a path is given as a percentage of the total distance between the two polyhedra at the extremes of that path. For practical purposes we arbitrarily consider deviations larger than 15% to be too large to consider a structure to belong to the interconversion path. By using these tools, it becomes straightforward to determine that the coordination sphere of the Nd1 atom in a particular salt of the $[Nd(H_2O)_9]^{3+}$ cation[14] (Figure 2, right) lies approximately along the r-CSAPR/r-TCTPR interconversion pathway (Δ = 16%).

When dealing with large numbers of structures we have found that the analysis of the shape measures is best done by means of shape maps,[8,16] that is, scatterplots of the shape measures relative to two ideal polyhedra. As specific distortions appear in the shape maps as well defined lines, the position of a given molecule in the shape map offers us a good idea of the type of distortion that it presents, although this technique does not always give an unequivocal description of the distortion. A discussion of the advantages of using shape measures and maps instead of bond angles for shape classification has been presented elsewhere.[10]

Table 2. Reciprocal shape measures $S_P(T)$ (upper triangle) and minimal distortion interconversion angles θ_{PT} (lower triangle, in degrees) between the reference nine-vertex polyhedra (see Figure 2 and Table 1 for drawings and names).

	r-TCTPR	s-TCTPR	r-CSAPR	MFF	TDIC	s-CCU	HH	J-TC	HBPYR
r-TCTPR	0	1.0768	1.1686	2.0446	11.8244	11.0336	14.3595	18.4168	21.4911
s-TCTPR	5.9558	0	1.2952	2.0132	15.2054	10.3122	12.3359	14.5241	20.6959
r-CSAPR	6.2056	6.5348	0	0.8173	13.9245	9.5635	13.4187	17.3103	21.0819
MFF	8.2210	8.1571	5.1868	0	13.5508	9.6879	11.2289	16.5406	18.5860
TDIC	20.1123	22.9504	21.9099	21.5996	0	15.4194	9.3828	14.3480	16.4991
s-CCU	19.4006	18.7313	18.0142	18.1348	23.1215	0	6.4014	16.1482	15.3018
HH	22.2681	20.5624	21.4888	19.5784	17.8376	14.6557	0	12.6796	14.7666
J-TC	25.4134	22.4020	24.5859	23.9982	22.2586	23.6942	20.8608	0	20.5034
HBPYR	27.6190	20.6959	27.3324	25.5386	23.9653	23.0279	22.5990	26.9238	0

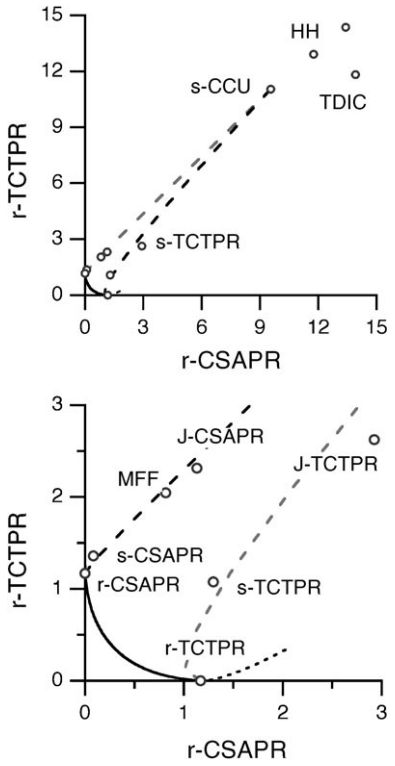

Figure 3. Shape map for ideal nine-vertex structures relative to the r-CSAPR and the r-TCTPR. The area corresponding to small values is shown in detail (right). Minimal distortion interconversion paths between the two ideal shapes (——) and from the CSAPR or the TCTPR to the s-CCU (– – –) are shown. An elongation of the TCTPR along its trigonal axis is shown by ——. ○ indicate the positions of other ideal structures in the shape map (see Figure 2 and Table 1).

For those readers not familiar with shape maps, analogies with road maps might be helpful. Thus, reference shapes are analogous to main cities, minimal distortion paths correspond to main roads between cities, and specific distorted structures are equivalent to small towns. With these analogies one can understand how to proceed to choose the two ideal shapes for a shape map. As there are $n(n-1)$ possible shape maps (in which n is the number of ideal shapes), we select a map in which the two cities closest to most of the towns we are interested in appear. This requires a previous analysis of the set of structures under analysis to find out which are the two most relevant shapes, that is, those for which most structures present small shape measures. In another respect, the representation of the minimal distortion path is useful even if the actual structures deviate significantly from that path, in the same way that the main highways are useful in a road map even when we are traveling to a small town that must be reached by a detour of a few kilometers by a side road.

For the subsequent discussion of experimental structural data we will mostly use a shape map relative to the two most common ideal structures in nine-coordinate complexes, the CSAPR and the TCTPR (Figure 3). The first feature to be noted is the small distance between the two ideal shapes considered, especially when compared with the corresponding distances between reference polyhedra of smaller coordination numbers (Table 3). Secondly, we can see that the capped cube (s-CCU), the J-TDIC, and the HH are geometrically far from the chosen reference shapes, whereas the alternative definitions of those reference shapes (s-CSAPR, J-CSAPR, s-TCTPR, and J-TCTPR) and the MFF are much closer. Finally, we must point out that the interconversion pathway between the TCTPR and the CSAPR proposed by Guggenberger and Muetterties[2] corresponds to a minimal distortion path in the sense of the continuous shape measures.

Table 3. Reciprocal shape measures of pairs of polyhedra with different numbers of vertices.

Vertices	Polyhedra	CShM
4	tetrahedron/square	33.33
6	octahedron/trigonal prism	33.33
7	capped octahedron/capped trigonal prism	1.53
7	pentagonal bipyramid/capped trigonal prism	6.64
8	triangular dodecahedron/square antiprism	2.85
9	tricapped trigonal prism/capped square antiprism	1.17

Overview of nine-coordinate transition-metal and rare-earth compounds: Most of the experimental data analyzed in this section were retrieved from the Cambridge Structural Database[17] (version 5.28) and from the Karlsruhe ICSD database (version 06-11-13) in searches for compounds with a metal atom belonging to periodic Groups 3–12 or to the lanthanide or actinide families and defined in the database as coordinated by nine donor atoms belonging to Groups 14–17. The following restrictions were applied: Hydride ligands were disregarded owing to the problems associated with locating them by X-ray crystallography in the vicinity of metal atoms (although we retained the homoleptic enneahydrido complexes because of their paradigmatic character) and no π-bonded ligands were allowed. To analyze separately homoleptic compounds with only monodentate ligands, we additionally restricted the metal–ligand bonds to acyclic ones. No restrictions were imposed regarding the existence of disorder or the values of the agreement factors R owing to the relatively small number of structures found. A total of 2075 crystallographically independent structural data sets were found. Of these, the largest proportion is provided by lanthanide compounds. Among the lanthanides, the largest number of nine-coordinate structures correspond to europium, gadolinium, neodymium, and lanthanum (Figure 4), and varying numbers of compounds were found for the rest of the lanthanides, except for the artificial promethium, for which no structure appears. Transition-metal compounds constitute only 6% of the nine-coordinate structures, most of which have yttrium as the central atom, with the rest distributed between cadmium, hafnium, nickel, scandium, tungsten, and zirconium. Barely 3% of nine-coordinate structures correspond to actinide compounds.

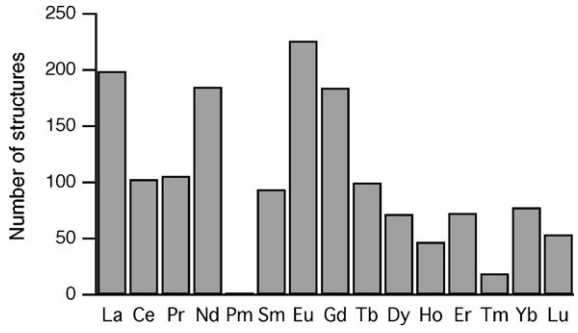

Figure 4. Distribution of structurally characterized nine-coordinate compounds of lanthanides, as found in the Cambridge Structural Database (version 5.28).

When analyzing a specific structure we can assign the polyhedron that best describes the coordination sphere of nine-coordinated metal atoms in each compound by calculating their CShMs relative to the various polyhedra sketched in Figure 2, and by taking as the coordination polyhedron the one that gives the smallest shape measure. However, if we wish to have a broad description of the structural preferences of nine-coordinated metal compounds, this approach is impractical because of their large stereochemical flexibility and the resulting dispersion of their shape measures relative to r-CSAPR and r-TCTPR (a shape map is provided in the Supporting Information, Figure D), that equally affects transition-metal, lanthanide, and actinide compounds. The situation does not improve if we analyze the data for compounds of the same metal, but some trends can be found if we group the complexes according to the nature of the coordinated ligands. We will start by looking at homoleptic compounds with monodentate ligands, free of the geometrical constraints imposed by bi- or multidentate ligands. Then we will discuss how some specific ligand topologies can control the stereochemical choice.

Monodentate ligands: We have found a total of 101 structural data sets of molecular compounds and 24 of extended solids in the family of homoleptic complexes with monodentate ligands. The molecular compounds include a large number of $[M(H_2O)_9]^{n+}$ complexes of scandium, yttrium, all lanthanides except promethium, and a few complexes with other ligands, such as oxide, fluoride, hydride, acetonitrile, ammonia, dimethyl sulfoxide, or dimethylformamide (for a full list of compounds and references see the Supporting Information, Table S1).

The shape measures of these compounds relative to r-TCTPR and r-CSAPR are presented in the shape map in Figure 5. A perspective view of the shape map clearly shows that most structures cluster around the two reference shapes, both for molecular compounds and for extended solids, even if a number of structures show significant distortions. As examples of the geometries found, we can pinpoint structure **a** in the map, which corresponds to an almost perfect r-CSAPR structure for the $[Pu(NCMe)_9]^{3+}$ ion (Figure 2, left) and the r-TCTPR shape for $[Sm(NCMe)_9]^{3+}$ (point **b** in Figure 5) whose structure is shown in Figure 6 (left). A third example is a structure that falls along the minimal distortion interconversion path between those two ideal shapes, $[Nd(H_2O)_9]^{3+}$ (point c in Figure 5), also shown in Figure 2 (right).

A few structures appear scattered along the paths to the CCU (Figure 5, top), among which the two uppermost

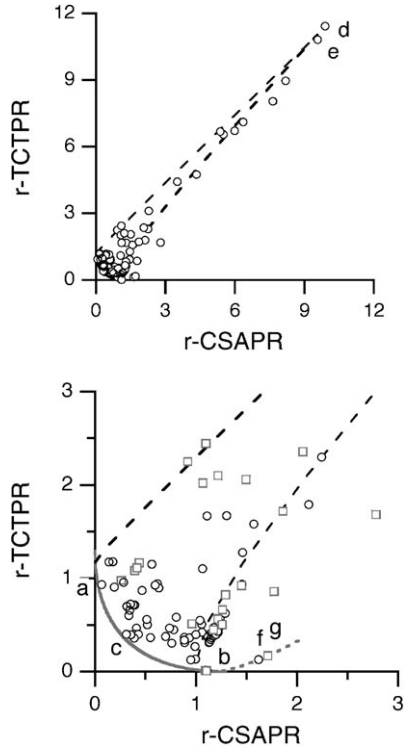

Figure 5. Shape map for homoleptic nine-coordinate complexes of transition metals and rare earths with monodentate ligands. In the large scale shape map shown below, ○: molecular compounds, □: extended solids (see Table S1 in the Supporting Information for more details).

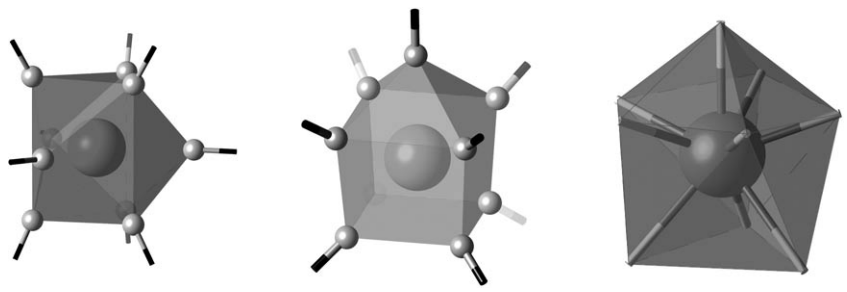

Figure 6. Coordination polyhedra of the lanthanide ion in the $[Sm(NCMe)_9]^{3+}$ (r-TCTPR, left)[27] and $[Pr(NCMe)_9]^{3+}$ (s-CCU, middle[28]) cations, and the MFF coordination polyhedron of rhenium in $[H_6Re(\mu\text{-}H)_3Re\{MeC(CH2_PPh_2)_3\}]^-$, determined by neutron diffraction at 80 K (right).[29]

points correspond to compounds whose geometries are very close to this polyhedron: The $[Pr(NCMe)_9]^{3+}$ cation[18] (Figure 5, top, point **e**) and the $[TaF_9]^{4-}$ ion[19] in Ba_3TaOF_9 (Figure 5, top, point **d**), as shown by their shape measures of 0.09 and 0.93 relative to s-CCU, respectively. The fact that the same praseodymium cationic complex appears in two other salts with the more usual TCTPR shape,[20] together with the molecular orbital criteria discussed below and the presence of disorder in the acetonitrile ligands, makes such an unusual structure worthy of reinvestigation. Other structures that seem to be intermediate between the square antiprism and the capped cube, with *S*(r-CSAPR) values higher than 4, are found to lie close to the minimal distortion interconversion path. One of these, the LaO_9 group[21] in $La_{1.7}Bi_{0.3}Mo_2O_9$, is closer to the TDIC, even if with a large value of the corresponding shape measure. Note that the lanthanum atoms in the $La_{2-x}Ba_xCuO_4$ superconducting phases are very well described by the CSAPR (shape measures between 0.7 and 1.1),[22] whereas the potassium site in the parent prototype K_2NiF_4 structure[23] is a significantly flattened r-CSAPR (shape measure of 2.6).

In the shape map we can see that some structures are intermediate between the two ideal shapes and close to the minimal distortion interconversion path. These structures can be identified by looking at the value of the path deviation function described above. In particular, one of the two crystallographically independent $[Nd(H_2O)_9]^{3+}$ ions in a co-crystal with a calixarene[24] appears practically in the middle of the interconversion path. The representation of its molecular structure (Figure 2, right) nicely shows how the same structure can be perceived visually either as a TCTPR or as a CSAPR owing to the small distance that separates these two ideal polyhedra in the space of continuous shape measures. To appreciate the two alternative descriptions one can focus either on the uppermost vertex, which should be regarded as the atom capping a square antiprism, or on one of the three atoms capping the rectangular faces of a trigonal prism, respectively.

From the analysis of the numerical values of the shape measures we have also been able to identify a number of structures that deviate from our ideal r-TCTPR shape, but are neatly aligned along the distortion path corresponding to an elongation of the trigonal prism along the trigonal axis, thus retaining the D_{3h} symmetry and varying only the edge ratios of the polyhedron. This is the case with the $[ReH_9]^{2-}$ anion in its barium salt[25] (Figure 5, bottom, point **f**) and with the LaF_9 groups[26] in $Na_3La_3F_{12}$ (Figure 5, bottom, point **g**). Still a significant number of structures are roughly aligned along the minimal distortion path for the interconversion of the r-TCTPR and r-CSAPR polyhedra, which suggests that these two shapes are quite similar in energy.

The preference of the homoleptic complexes for structures close to r-TCTPR or r-CSAPR is in agreement with qualitative arguments based both on minimum ligand–ligand repulsion schemes and optimum metal–ligand bonding. Hence, based on a limited number of structures available at that time, Guggenberger and Muetterties found that nine-coordinated metal centers in discrete molecules and in edge-sharing linear chain compounds show little deviation from the TCTPR.[2] These authors calculated point-charge repulsion energies and concluded that such a geometry is more stable than the CSAPR. They pointed out, however, that some coordination compounds with chelating ligands may favor distortion of the TCTPR shape towards the CSAPR. Kepert,[30] using a similar model, analyzed five nine-vertex geometries (TCTPR, CSAPR, CCU, TDIC, and TC) and showed that the last three shapes have large ligand–ligand repulsion coefficients. From a molecular orbital point of view, an easy way to discriminate those coordination geometries that are expected to be more stable is to determine for each coordination polyhedron whether there is a symmetry match between the atomic orbitals of the central metal atom and the symmetry-adapted linear combinations of the σ-donor orbitals of the ligands or not.[31] In the case of nine-coordinate complexes, there must be a symmetry match for each one of the nine valence atomic orbitals so as to form nine metal–ligand bonding and nine antibonding molecular orbitals. In such cases, a maximum bonding interaction can be achieved and the corresponding coordination geometry is expected to be a common one. For those cases in which at least one atomic orbital (or equivalently, one symmetry-adapted combination of ligand σ-donor orbitals) is nonbonding by symmetry, then the bond energy associated with those geometries should be expected to be smaller, and consequently, they are expected to correspond to high-energy shapes.

The first condition for an optimum metal–ligand bonding symmetry analysis commented upon in the previous paragraph is that the ligands must be distributed in almost a spherical fashion. Otherwise some metal atomic orbitals would be oriented towards a region of the space in which there are no metal–ligand interactions and a less effective bonding situation should occur. Accordingly, we have disregarded the hemispherical J-TC for our symmetry analysis. It is found that both CSAPR and TCTPR coordination geometries present a perfect symmetry match between the nine metal atomic orbitals available for bonding (disregarding the f orbitals for rare-earth metals because of their minor participation in metal–ligand bonding) and the nine symmetry-adapted linear combinations of ligand σ orbitals. These results can be illustrated in a semiquantitative way by means of the angular overlap model,[32] as seen in Figure 7. A similar situation is found for the MFF and TDIC shapes, whereas the three remaining polyhedra (CCU, HBPYR, and HH) leave one or more d orbitals as nonbonding, which results in much less efficient metal–ligand bonding. For instance, the CCU leaves the d_{xy} orbital (B_1 representation in the C_{4v} symmetry point group) as strictly nonbonding and the HBPYR geometry leaves the e_{1g} degenerate pair of orbitals d_{xz} and d_{yz} (D_{7h} point group) as nonbonding. In summary, we expect the CSAPR, TCTPR, MFF, and TDIC shapes to be predominant in nine-coordinate systems, whereas all other geometries considered are much less likely to appear

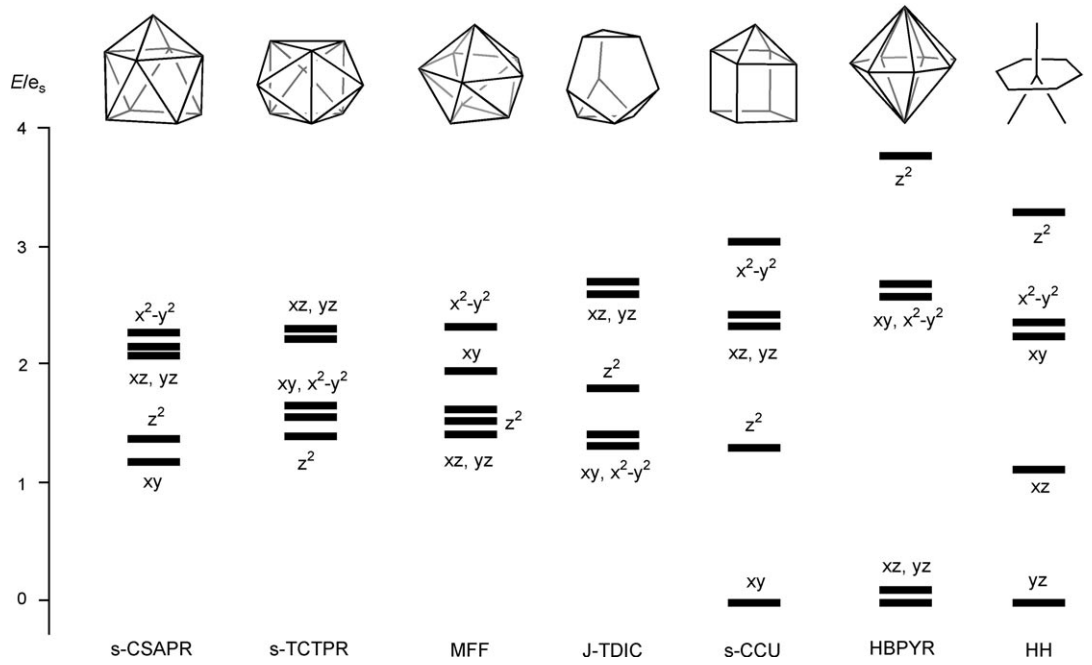

Figure 7. Splitting pattern for the d orbitals in several nine-vertex polyhedral structures, in accordance with the angular overlap model (see Table 1 for abbreviations).

unless required by the stereochemical constraints imposed by rigid multidentate ligands.

Stereochemical preferences by ligand

Four oxalato ligands: In this section we consider those complexes with four bidentate oxalato ligands, a family with a significant number of members. The shape measures for the coordination spheres of these compounds are plotted in the shape map shown in Figure 8. There it can be seen that, with two exceptions, all of the structures are roughly aligned along the r-CSAPR/r-TCTPR interconversion path, most of them closer to the CSAPR than to the TCTPR. Two outliers clearly show up in Figure 8, which correspond to guanidinium clathrates of oxalato-bridged networks of neodymium[33] or lanthanum.[34] However, we have found neither chemically nor crystallographically distinctive features in these compounds that could account for their different stereochemistry. For instance, a similar guanidinium and ammonium clathrate of the neodymium oxalato compound[34] adheres to the general trend. The arrangement of the four bidentate ligands along the polyhedral edges is quite variable and include CSAPRs with conformations **1**,[35] **2**,[36] **3**,[37] or **4**,[35,38] and TCTPRs **6**,[39] or **7**.[40]

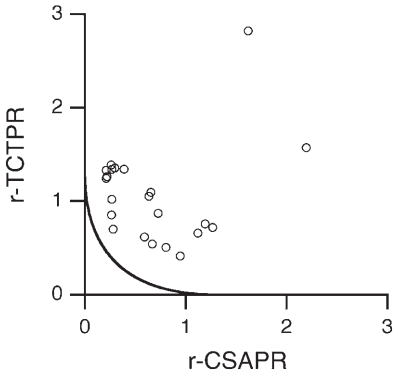

Figure 8. Shape map for compounds of the type $[M(oxalato)_4L]$. ○ correspond to the experimental structures and —— is the minimal distortion interconversion path between the r-TCTPR and r-CSAPR reference polyhedra.

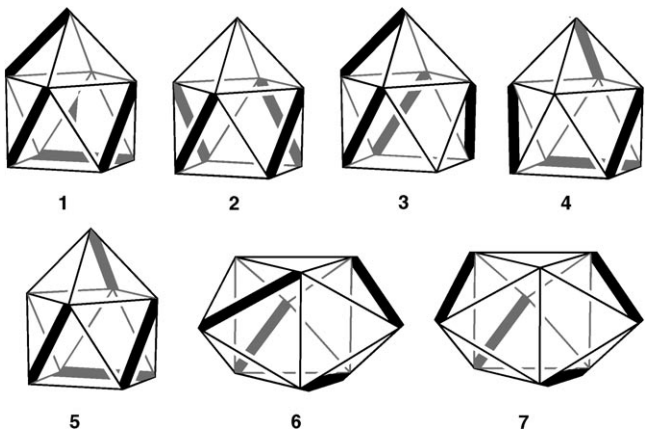

Three bidentate ligands: In this family we consider those complexes with three bidentate and three monodentate ligands in which the bidentate ligands can form four- (nitrates, sulfate, and carboxylate), five- (ethylenediamine, oxalate, and topologically equivalent ligands), or six-membered

chelate rings (β-diketonates). Representation of these structures in a r-CSAPR/r-TCTPR shape map (Figure 9) clearly shows that the small bite ligands result in severely distorted polyhedra, whereas those ligands that form five- or six-membered chelate rings may appear closer to the interconversion path between the two reference polyhedra.

A look at the structures that are close to the reference

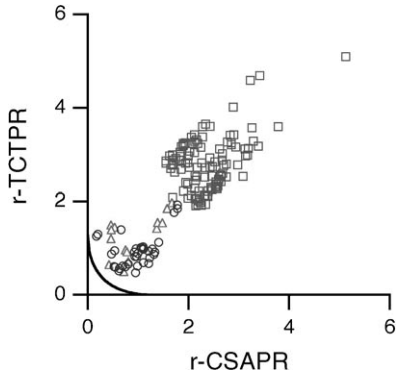

Figure 9. Shape map for tris(chelate) nine-coordinate complexes of transition metals and lanthanides forming four- (nitrato ligands, □), five- (○), or six-membered (β-diketonato ligands, △) chelate rings (for more details see the Supporting Information, Table S2). —— represents the minimal distortion interconversion path between the CSAPR and the TCTPR.

shapes reveals a variety of arrangements of the three chelate rings on the coordination polyhedra. In the presence of the ligands with the smallest bite we have identified conformations **8**[41] and **9**[42] close to the CSAPR, and conformation **10** close to the TCTPR.[43]

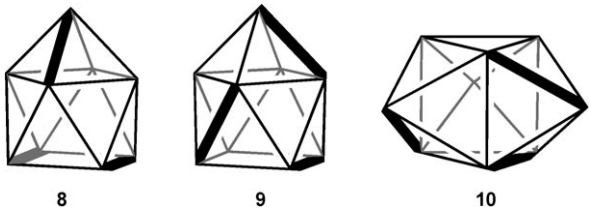

Three tridentate ligands: We use the term "clamps" to describe those tridentate ligands whose donor atoms are roughly arranged in a semicircle (**11**), such as terpyridine, and coordinate to a metal atom in a coplanar way. In contrast, "grasping" tridentate ligands (**12**) are those in which the three donor atoms are regularly arranged in a circle, but that coordinate to a metal atom in a noncoplanar way, two typical examples of which are tris(pyrazolyl)borate and triazacyclononane. In this section we present the results of our shape analysis for complexes of the type $[M(clamp)_3]$.

In this family, the geometries of the coordination spheres are much closer to TCTPR than to CSAPR. Furthermore, deviations from that ideal polyhedron correspond to distortions towards the TDIC rather than towards CSAPR. This can be clearly appreciated in the s-TCTPR/J-TDIC shape

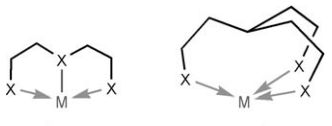

11 **12**

map (Figure 10). Note that in this case the TCTPR that best describes the experimental structures is a spherical version in which the lateral faces of the trigonal prism are squares rather than rectangles. This geometry is unfavorable for complexes with monodentate ligands because of the shorter ligand–ligand distance between the capping and basal coordination sites, but is favored by clamp ligands precisely because of the shorter donor–donor distance of the chelate rings.

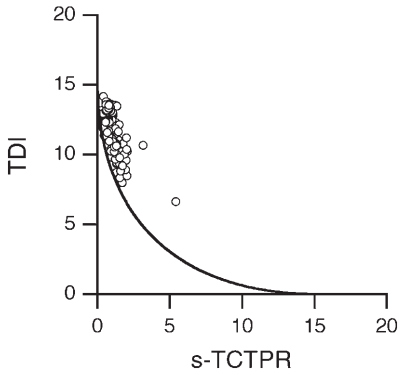

Figure 10. Shape map for the $[M(clamp)_3]$ complexes relative to the s-TCTPR and J-TDIC reference polyhedra (see the Supporting Information, Table S3, for more details). —— represents the minimal distortion interconversion path between the two reference shapes.

In all of these complexes, the clamp ligands are arranged in a helical manner (**13**) as noted earlier by Drew,[3] each one decorating one of the square faces of the trigonal prism, as illustrated by the example shown in Figure 11.[44] In spite of the helical nature of these complexes, none has crystallized in an enantiomorphic space group and the two enantiomers are, therefore, present in achiral solids.

Five complexes found with three tris(pyrazolyl)borato ligands[45,46] all present an almost perfect s-TCTPR structure with shape measures of less than 0.2. In each case, each ligand occupies one of the capping vertices and one vertex of each of the triangular bases (**14**), as shown for $[Pr(tpb)_3]$[45] in Figure 12.

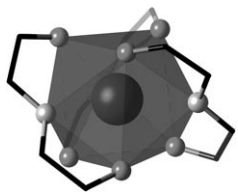

Figure 11. Coordination sphere of the lutetium atom in the $[Lu(1,3\text{-pyridinetricarboxylato})_3]^{3-}$ ion,[44] which shows the helical arrangement of the tridentate ligands, also represented by schematic version **13**.

Branched multidentate ligands: We have examined a variety of multidentate ligands with differ-

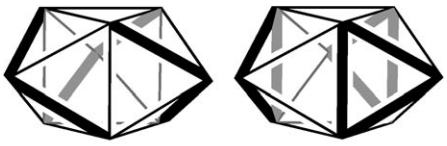

13 14

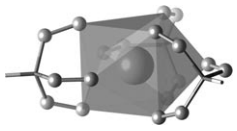

Figure 12. Coordination sphere of the metal atom in [Pr(tpb)$_3$], which shows the helical arrangement of the tridentate ligands, also represented by schematic version **14**.

ent branching schemes and denticities, with their topologies illustrated by **15**. All of these compounds behave similarly to monodentate ligands and have structures close to the CSAPR and the TCTPR, but well separated from the interconversion path, most likely because of the constraints imposed by the chelate rings. Apparently, these ligands are flexible enough to adopt geometries close to the electronically preferred polyhedra.

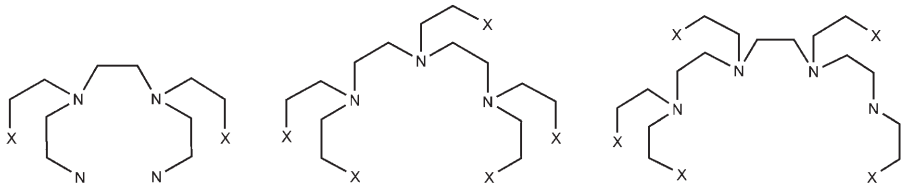

15

Hexadentate macrocyclic ligands: Hexadentate macrocyclic ligands, such as the O_6-crown ethers shown in the projection in **16**, can in principle occupy six almost coplanar coordination positions in [M(O_6-crown)L_3] complexes, which requires the three additional ligands to coordinate asymmetrically on either side of the crown ether. The idealized representation of the metal, the three monodentate ligands, and the macrocyclic ring could be described as like a child playing with a hula hoop (Figure 13). The relative orientation of the hula hoop and the feet of the child can be eclipsed (**16a**) or staggered (**16b**), or at any intermediate orientation. In the eclipsed conformation, the irregular coordination polyhedron is formed by ten triangular and two tetragonal faces, whereas in the staggered conformation it has fourteen triangular faces. The best examples of these two polyhedra are represented in Figure 13. In spite of the differences between these two HH polyhedra, they are rather similar in the CShM space (1.38) and we will consider only the eclipsed one as a reference polyhedron for simplicity.

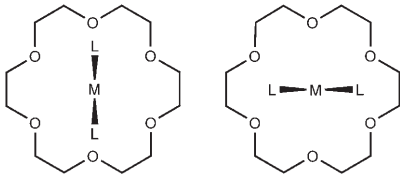

16a 16b

The analysis of the structures of complexes with hexadentate macrocyclic ligands is best done by plotting their shape measures on an HH/r-CSAPR shape map (Figure 14). There it can be seen that all of the structures are virtually aligned along the minimal distortion interconversion path. Minor deviations from the interconversion path are as a result of a slight deviation of the six donor atoms from planarity, and also deviations of the structures from the ideal eclipsed conformation owing to the unhindered rotation of the ring around the central ML_3 unit. Note that the distribution of this family of structures is much closer to the CSAPR than to the HH. As an example, we show in Figure 15 the coordination sphere of the ytterbium atom in [Yb(O_4N_2-macrocycle)$(SCN)_3$][49] in which the macrocycle encircles the metal atom occupying the capping coordination site, two sites of the upper face of the square antiprism, and three sites at the base. Our qualitative orbital analysis above (Figure 7) showed that the HH shape is unfavorable for metal–ligand bonding, a prediction that is supported by the fact that it is only found in this family of compounds in which six donor atoms are forced to remain almost coplanar because of the macrocyclic nature of the hexadentate ligand. We have seen above that complexes with analogous open-chain hexadentate ligands are not even close to the HH shape.

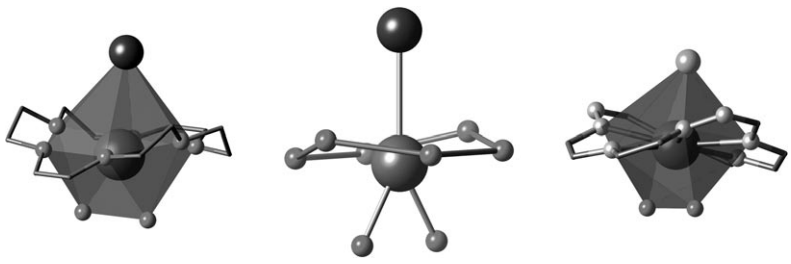

Figure 13. Perspective view of the crown ether and the coordination sphere of the lanthanum ions in [I(dibenzo[18]crown-6)La(μ-OH)$_2$La(dibenzo[18]crown-6)I][47] with an eclipsed conformation (left), its idealized version reminiscent of a hula hoop player (middle), and the coordination sphere of the europium atom in a complex with a macrocyclic hexadentate nitrogen donor ligand (right).[48]

Tetrapodal octadentate ligands: A good number of nine-coordinate complexes have been reported with octadentate ligands

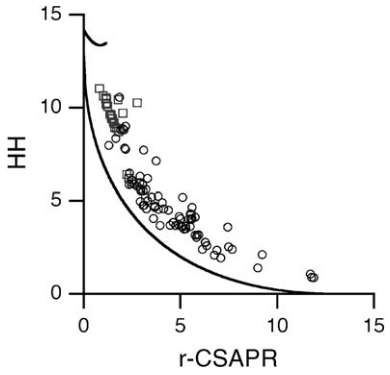

Figure 14. Shape map for the complexes with hexadentate macrocyclic (○) and related open-chain hexadentate ligands (□) relative to the r-CSAPR and the HH shapes, together with the minimal distortion interconversion pathway (solid line). The short line at the top left corresponds to the r-CSAPR/r-TCTPR pathway.

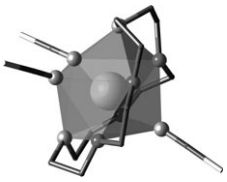

Figure 15. Perspective view of the hexadentate macrocyclic ligand and of the approximately square antiprismatic coordination sphere of the ytterbium atom in $[Yb(O_4N_2\text{-macrocycle})(SCN)_3]$.[49]

based on tetraazacyclododecane to which four arms with a donor atom have been added, such as (2-hydroxyethyl)-1,4,7,10-tetraazacyclododecane (**18**). In keeping with the tetragonal symmetry of these ligands, their coordination spheres are much closer to the CSAPR than to the TCTPR. Therefore, for this family it is appropriate to use a shape map relative to the two tetragonal reference geometries, the r-CSAPR and the s-CCU (Figure 16). In this shape map we see that the experimental structures appear nicely aligned along the interconversion pathway, as quantified by path deviation functions of less than 15%, with one exception that has a deviation of 20%. Furthermore, the structures form two distinct groups. Out of the 82 data sets found for 60 chemical compounds, 54 present similar distortions of at most 30% from the CSAPR with little dispersion in their generalized interconversion coordinates. The rest of the structures are spread along the minimal distortion path, with degrees of conversion towards the s-CCU of between 35 and 80%. All the structures that are close to the CSAPR have either carboxylato or amido groups on their four arms,[50] although similar complexes also appear in the group of distorted structures. On the other hand, all of the complexes with 2-hydroxyethyl arms (such as **18**) are distorted to different degrees towards the s-CCU.[51] We have found no correlation between the bite of the tetrapodal ligands and their degree of distortion from the CSAPR.

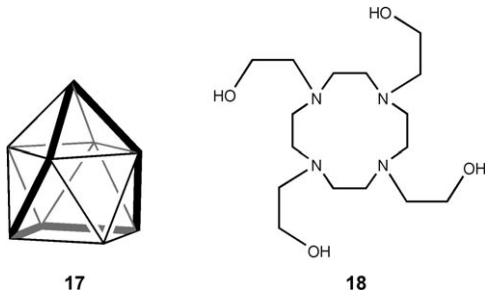

17 **18**

Nonadentate tentacular and encapsulating ligands: Several three-legged nonadentate ligands have been designed in which the three legs can end in a triazacyclononane (**19**)[52] or in an sp^3 carbon or nitrogen atom in tentacular ligands (**20**),[53] or can be wrapped to form encapsulating ligands (**21**).[54] The structural data for these families of compounds are represented in the shape map shown in Figure 17, which

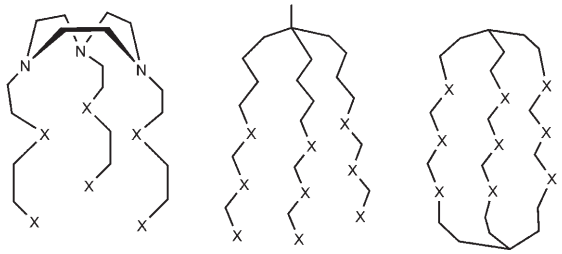

19 **20** **21**

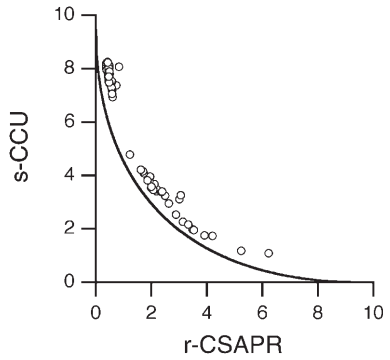

Figure 16. Shape map for nine-coordinate complexes with octadentate tetrapodal ligands based on tetraazacyclododecane (**18**) relative to the r-CSAPR and the s-CCU. —— corresponds to the minimal distortion path for the interconversion of the two reference shapes.

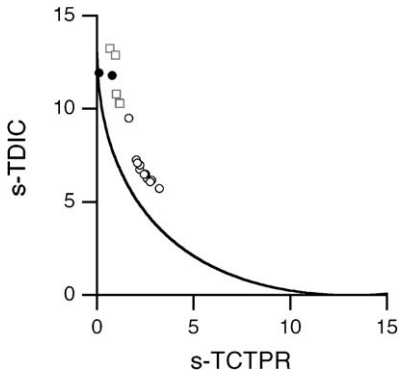

Figure 17. Shape map for nine-coordinate complexes with nonadentate extended tripod ligands based on triazacyclononane (**19**, ○), tentacular ligands (**20**, □) and encapsulating ligands (**21**, ●) relative to the s-TCTPR and the s-TDIC.

nicely shows that such ligands force an approximately trigonal symmetry and deviations from TCTPR are essentially aligned along the distortion path to TDIC, even if no structure gets close to having this shape.

Conclusion

The nine-coordinated metal centers with mono- and bidentate ligands tend to adopt structures close to r-TCTPR or to r-CSAPR with a large stereochemical variability that suggests a rather shallow potential energy surface. Similar behavior has been found for open-chain, branched multidentate ligands that are flexible enough to adapt to the electronic preference for these two reference shapes.

The use of more rigid multidentate ligands, however, can enforce specific coordination geometries that are rarely met by the simpler ligands. The positions of the structures analyzed in several shape maps can be schematically summarized in a topological map (Figure 18) that shows us which polyhedra and interconversion path are obtained with each type of ligand. Therefore, compounds with three tridentate grasping ligands (**12**), which are all close to the r-TCTPR shape, are represented by a circle beside the corresponding polyhedral symbol. Other families of compounds that appear scattered along the interconversion path between two ideal polyhedra are represented by a band joining the corresponding polyhedra. In some cases, the structures may be found to be distorted towards a certain polyhedron, but without ever coming close to its shape, a fact that is represented by a band shorter than the full path. Furthermore, the dispersion of the shapes of a given family away from the path is roughly represented by the width of the band. In this way we can see in Figure 18 that complexes with tetrapodal ligands are capped square pyramids with varying degrees of distortion towards the CCU, whereas complexes with hexadentate macrocyclic ligands are distorted towards the HH geometry. Finally, complexes with tentacular nonadentate ligands are tricapped trigonal prismatic with distortions towards the TDIC, and the same distortion to a somewhat lesser degree is found in complexes with three clamp tridentate ligands.

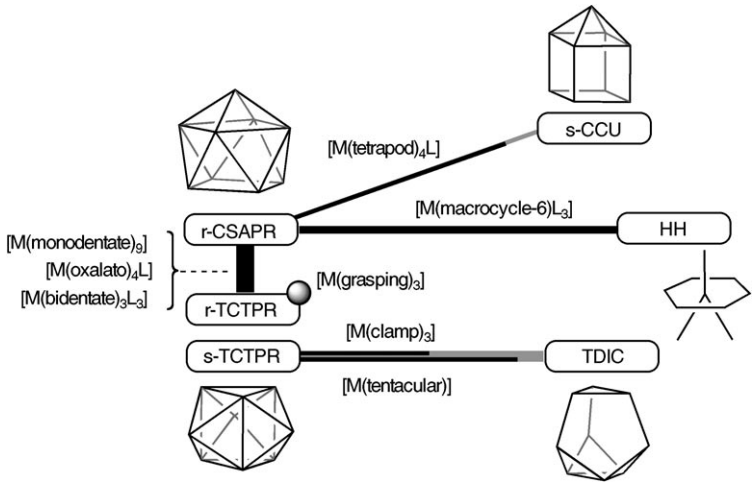

Figure 18. Schematic shape atlas for several families of nine-coordinate compounds classified by ligands. A circle indicates shapes very close to the corresponding polyhedron and black bars indicate structures scattered along a polyhedral interconversion pathway (background grey bars) with the width of the bar roughly indicating the degree of deviation from the path.

Acknowledgements

Support from the Dirección General de Investigación (MEC, project no. CTQ2005-08123-C02-02BQU) and from the Comissió Interdepartamental de Ciència i Tecnologia (CIRIT, grant no. 2005SGR-00036) is gratefully acknowledged.

[1] D. L. Kepert, *Inorganic Stereochemistry*, Springer, New York, **1982**.
[2] L. J. Guggenberger, E. L. Muetterties, *J. Am. Chem. Soc.* **1976**, *98*, 7221.
[3] M. G. B. Drew, *Coord. Chem. Rev.* **1977**, *24*, 179.
[4] N. W. Johnson, *Canad. J. Math.* **1966**, *18*, 169; P. R. Cromwell, *Polyhedra*, Cambridge University Press, Cambridge, **1997**; S. Alvarez, *Dalton Trans.* **2005**, 2209.
[5] H. Zabrodsky, S. Peleg, D. Avnir, *J. Am. Chem. Soc.* **1992**, *114*, 7843.
[6] M. Pinsky, D. Avnir, *Inorg. Chem.* **1998**, *37*, 5575.
[7] J. Cirera, P. Alemany, S. Alvarez, *Chem. Eur. J.* **2004**, *10*, 190.
[8] S. Alvarez, D. Avnir, M. Llunell, M. Pinsky, *New J. Chem.* **2002**, *26*, 996.
[9] D. Casanova, J. M. Bofill, P. Alemany, S. Alvarez, *Chem. Eur. J.* **2003**, *9*, 1281.
[10] D. Casanova, M. Llunell, P. Alemany, S. Alvarez, *Chem. Eur. J.* **2005**, *11*, 1479.
[11] H. Zabrodsky, S. Peleg, D. Avnir, *J. Am. Chem. Soc.* **1993**, *115*, 7843.
[12] D. Casanova, J. Cirera, M. Llunell, P. Alemany, D. Avnir, S. Alvarez, *J. Am. Chem. Soc.* **2004**, *126*, 1755.
[13] We adopt here the names commonly used in chemistry, but we note that the Johnson systematic names for the first three polyhedra are elongated square pyramid (capped cube), gyroelongated square pyramid (capped square antiprism), and triaugmented trigonal prism (tricapped trigonal prism).
[14] S. J. Dalgarno, J. L. Atwood, C. L. Raston, *Cryst. Growth Des.* **2006**, *6*, 174.
[15] A. E. Enriquez, J. H. Matonic, B. L. Scott, M. P. Neu, *Chem. Commun.* **2003**, 1892.
[16] S. Alvarez, P. Alemany, D. Casanova, J. Cirera, M. Llunell, D. Avnir, *Coord. Chem. Rev.* **2005**, *249*, 1693.
[17] F. H. Allen, O. Kennard, *Chem. Des. Autom. News* **1993**, *8*, 31.
[18] G. R. Willey, D. R. Aris, W. Errington, *Inorg. Chim. Acta* **2001**, *318*, 97.
[19] M. P. Crosnier-Lopez, H. Duroy, J. L. Fourquet, Y. Lalignant, *Eur. J. Solid State Inorg. Chem.* **1995**, *92*, 457.
[20] G. R. Willey, D. R. Aris, W. Errington, *Inorg. Chim. Acta* **2001**, *318*, 97; G. B. Deacon, B. Gortler, P. C. Junk, E. Lork, R. Mews, J. Petersen, B. Zemva, *J. Chem. Soc., Dalton Trans.* **1998**, 3887.
[21] I. P. Marozau, A. L. Shaula, V. V. Kharton, N. P. Vyshatko, A. P. Viskup, J. R. Frade, F. M. B. Mar-

ques, *Mater. Res. Bull.* **2005**, *40*, 361.
[22] S. Katano, J. A. Fernández-Baca, S. Funahashi, N. Mori, Y. Ueda, K. Koga, *Phys. C (Amsterdam, Neth)* **1993**, *214*, 64; M. Ferretti, E. Magnone, M. Napoletano, *Int. J. Mod. Phys. B* **1999**, *13*, 979.
[23] D. Balz, K. Plieth, *Z. Elektrochem.* **1953**, *59*, 545; D. Babel, E. Herdtweck, *Z. Anorg. Allg. Chem.* **1982**, *487*, 75; S. K. Yeh, S. Y. Wu, C.-S. Lee, Y. Wang, *Acta Crystallogr., Sect. A* **1993**, *49*, 806.
[24] S. J. Dalgarno, M. J. Hardie, C. L. Raston, *Cryst. Growth Des.* **2004**, *4*, 227.
[25] N. T. Stetson, K. Yvon, P. Fischer, *Inorg. Chem.* **1994**, *33*, 4598.
[26] W. H. Zachariasen, *Acta Crystallogr.* **1948**, *1*, 265.
[27] G. B. Deacon, B. Gortler, P. C. Junk, E. Lork, R. Mews, J. Petersen, B. Zemva, *J. Chem. Soc., Dalton Trans.* **1998**, 3887.
[28] G. R. Willey, D. R. Aris, W. Errington, *Inorg. Chim. Acta* **2001**, *318*, 97.
[29] S. C. Abrahams, A. P. Ginsberg, T. F. Koetzle, P. Marsh, C. R. Sprinkle, *Inorg. Chem.* **1986**, *25*, 2500.
[30] D. L. Kepert, *Prog. Inorg. Chem.* **1981**, *28*, 309.
[31] J. Cirera, S. Alvarez, *Angew. Chem. Int. Ed.* **2006**, *45*, 3012; *Angew. Chem.*, **2006**, *118*, 3078.
[32] E. M. Larsen, G. N. LaMar, *J. Chem. Educ.* **1974**, *51*, 633; J. K. Burdett, *Molecular Shapes*, Wiley, New York, **1980**.
[33] J.-C. Trombe, A. Mohanu, *Solid State Sci.* **2004**, *6*, 1403.
[34] F. Fourcade-Cavillou, J.-C. Trombe, *Solid State Sci.* **2002**, *4*, 1199.
[35] B. Chapelet-Arab, G. Nowogrocki, F. Abraham, S. Grandjean, *J. Solid State Chem.* **2005**, *178*, 3055.
[36] H. Steinfink, G. D. Brunton, *Inorg. Chem.* **1970**, *9*, 2112; T. Bataille, D. Louer, *Acta Crystallogr., Sect. C: Cryst. Struct. Commun.* **1999**, *55*, 1760.
[37] Y.-Y. Yang, S.-B. Zai, W.-T. Wong, S. W. Ng, *Acta Crystallogr., Sect. E: Struct. Rep. Online* **2005**, *61*, m1912.
[38] R. Vaidhyanathan, S. Natarajan, C. N. R. Rao, *Chem. Mater.* **2001**, *13*, 185.
[39] J.-L. Song, J.-G. Mao, *Chem. Eur. J.* **2005**, *11*, 1417; R. Vaidhyanathan, S. Natarajan, C. N. R. Rao, *Inorg. Chem.* **2002**, *41*, 2202.
[40] I. A. Kahwa, F. R. Fronczek, J. Selbin, *Inorg. Chim. Acta* **1984**, *82*, 161.
[41] J.-K. Tang, Y.-Z. Li, Q.-L. Wang, E.-Q. Gao, D.-Z. Liao, Z.-H. Jiang, S.-P. Yan, P. Cheng, L.-F. Wang, G.-L. Wang, *Inorg. Chem.* **2002**, *41*, 2188.
[42] X. Zhang, Y. Cui, F. Zheng, J. Huang, *Chem. Lett.* **1999**, 1111.
[43] C. Papadimitriou, P. Veltisistas, J. Marek, J. D. Woollins, *Inorg. Chim. Acta* **1998**, *267*, 299.
[44] P. A. Brayshaw, A. K. Hall, W. T. A. Harrison, J. M. Harrowfield, D. Pearce, T. M. Shand, B. W. Skelton, C. R. Whitaker, A. H. White, *Eur. J. Inorg. Chem.* **2005**, 1127.
[45] C. Apostolidis, J. Rebizant, B. Kanellakopulos, R. V. Ammon, E. Dornberger, J. Muller, B. Powietzka, B. Nuber, *Polyhedron* **1997**, *16*, 1057.
[46] H. Reddmann, C. Apostolidis, O. Walter, J. Rebizant, H.-D. Amberger, *Z. Anorg. Allg. Chem.* **2005**, *631*, 1487; C. Apostolidis, J. Rebizant, O. Walter, B. Kanellakopulos, H. Reddmann, H.-D. Amberger, *Z. Anorg. Allg. Chem.* **2002**, *628*, 2013.
[47] C. Runschke, G. Meyer, *Z. Anorg. Allg. Chem.* **1997**, *623*, 1493.
[48] R. Haner, J. Hall, G. Rihs, *Helv. Chim. Acta* **1997**, *80*, 487.
[49] F. Benetollo, G. Bombieri, G. Depaoli, M. R. Truter, *Inorg. Chim. Acta* **1996**, *245*, 223.
[50] S. Aime, A. S. Batsanov, M. Botta, J. A. K. Howard, M. P. Lowe, D. Parker, *New J. Chem.* **1999**, *23*, 669; G. Zucchi, A.-C. Ferrand, R. Scopelliti, J.-C. G. Bunzli, *Inorg. Chem.* **2002**, *41*, 2459; T. Gunnlaugsson, R. J. H. Davies, M. Nieuwenhuyzen, J. E. O'Brien, C. S. Stevenson, S. Mulready, *Polyhedron* **2003**, *22*, 711; S. Aime, A. Barge, M. Botta, J. A. K. Howard, R. Kataky, M. P. Lowe, J. M. Moloney, D. Parker, A. S. Sousa, *Chem. Commun.* **1999**, 1047.
[51] R. U. Richards-Johnson, I. A. Kahwa, A. J. Lough, *Acta Crystallogr., Sect. E: Struct. Rep. Online* **2003**, *59*, m1022; M. K. Thompson, A. J. Lough, A. J. P. White, D. J. Williams, I. A. Kahwa, *Inorg. Chem.* **2003**, *42*, 4828.
[52] L. Tei, A. J. Blake, M. W. George, J. A. Weinstein, C. Wilson, M. Schroder, *Dalton Trans.* **2003**, 1693; C. Gateau, M. Mazzanti, J. Pécaut, F. A. Dunand, L. Helm, *Dalton Trans.* **2003**, 2428; L. Tei, G. Baum, A. J. Blake, D. Fenske, M. Schroder, *J. Chem. Soc., Dalton Trans.* **2000**, 2793; L. Tei, A. J. Blake, C. Wilson, M. Schroder, **2004**; L. Charbonniere, R. Ziessel, M. Guardigli, A. Roda, N. Sabbatini, M. Cesario, *J. Am. Chem. Soc.* **2001**, *123*, 2436.
[53] S. Koeller, G. Bernardinelli, B. Bocquet, C. Piguet, *Chem. Eur. J.* **2003**, *9*, 1062; S. Koeller, G. Bernardinelli, C. Piguet, *Dalton Trans.* **2003**, 2395; Y. Bretonniere, R. Wietzke, C. Lebrun, M. Mazzanti, J. Pecaut, *Inorg. Chem.* **2000**, *39*, 3499.
[54] X.-L. Hu, Y.-Z. Li, Q.-H. Luo, *Polyhedron* **2004**, *23*, 49; X.-L. Hu, Y.-Z. Li, Q.-H. Luo, *J. Coord. Chem.* **2003**, *56*, 1277.

Received: July 24, 2007
Published online: November 14, 2007

